

Variational Analysis of Oversampled Dual-Doppler Radial Velocity Data and Application to the Analysis of Tornado Circulations

MING XUE

Center for Analysis and Prediction of Storms, and School of Meteorology, University of Oklahoma, Norman, Oklahoma

SHUN LIU

Center for Analysis and Prediction of Storms, University of Oklahoma, Norman, Oklahoma, and College of Atmospheric Science, Lanzhou University, Lanzhou, China

TIAN-YOU YU

School of Electrical and Computer Engineering, University of Oklahoma, Norman, Oklahoma

(Manuscript received 17 March 2006, in final form 7 June 2006)

ABSTRACT

For the detection of severe weather phenomena such as tornados, mesocyclones, and strong wind shear, the azimuthal resolution of radial velocity measurements is more important. The typical azimuthal resolutions of 1° for the Weather Surveillance Radar-1988 Doppler (WSR-88D) radars and of 2° for the planned Center for Collaborative Adaptive Sensing of Atmosphere (CASA) radars are not sufficient for this purpose, especially at far ranges. Oversampling is one strategy that can potentially provide more details about the azimuthal structures of flows, and can be achieved by processing raw data at azimuthal increments smaller than the radar beamwidth. In the presence of dual-Doppler observations, the variational method can be used to effectively recover subbeamwidth structures from these oversampled data, which, combined with the typically higher range resolutions, can provide high-resolution wind analyses that are valuable for, for example, tornado detection. This idea is tested in this paper using simulated data as well as reprocessed level-I data from a research WSR-88D radar, for model-simulated and actually observed tornadoes, respectively. The results confirm that much more detailed, often subbeamwidth, flow structures can indeed be recovered through azimuthal oversampling and a properly configured variational analysis, and the detailed flow analysis is expected to significantly improve one's ability in identifying small-scale features such as tornadoes from radial velocity observations.

1. Introduction

The newly established National Science Foundation (NSF) Engineering Research Center (ERC) for Collaborative Adaptive Sensing of the Atmosphere (CASA) is to develop innovative observing systems for high-resolution sensing of the lower atmosphere. The development of low-cost, high-density (also short range), and dynamically adaptive networks of Doppler radars is the key to its success (e.g., Xue et al. 2006). The range resolution of the CASA radars to be de-

ployed in the Oklahoma test bed (Brotzge et al. 2005) is as high as 100 m; the azimuthal resolution, defined by the half-power beamwidth, is designed to be 2° to keep the hardware cost down.

For the purpose of detecting hazard weather such as tornado and strong wind shear, the azimuthal resolution is most important. The 2° azimuthal resolution may not be sufficient for tornado detection, especially for smaller tornadoes at far ranges (May et al. 2006, manuscript submitted to *J. Atmos. Oceanic Technol.*). On the other hand, the average spacing of approximately 30 km between the CASA radars allows for good dual- or possibly multi-Doppler radar coverage within the network. This provides us with an opportunity to explore various scanning strategies that would allow for better retrieval of subbeamwidth flow structures. In this pa-

Corresponding author address: Ming Xue, Center for Analysis and Prediction of Storms, National Weather Center, Suite 2500, 120 David L. Boren Blvd, Norman, OK 73072.
E-mail: mxue@ou.edu

per, a novel method is proposed, in which azimuthal oversampling is performed by two Doppler radars and the oversampled radial velocity data are then analyzed using a variational method to retrieve subbeamwidth flow structures. The technique also provides us with an analysis of the complete wind field from which diagnostic quantities, such as vorticity and divergence, can be readily calculated and also used to initialize very high-resolution numerical models.

The three spectral moments commonly used by meteorological applications are the reflectivity factor, mean radial velocity, and spectrum width. For the Weather Surveillance Radar-1988 Doppler (WSR-88D) radars, they are defined as level-II data (Crum et al. 1993). The moment data are often obtained by processing a number of raw data samples termed level-I data using the autocovariance method (Doviak and Zrnic 1993). For WSR-88D as well as the initial Oklahoma test bed CASA radars, mechanically rotating antennas are used. The antenna motion will produce azimuthal smearing so that the effective beamwidth is wider than the physical beamwidth. Moreover, the resolution volumes of individual samples are continuously shifted in azimuth (Doviak and Zrnic 1993; Wood and Brown 1997).

A Gaussian-shaped antenna pattern is often assumed in the azimuthal direction (e.g., Wood and Brown 1997), which neglects the effect of sidelobes. The effective beamwidth of the Gaussian will become broader due to the antenna motion and is a function of the number of samples used, antenna's rotation rate, and the pulse repetition time. Oversampling in azimuth can be achieved by estimating the spectral moments over a smaller number of samples or by rotating the antenna more slowly to obtain a sufficient number of samples for the required data accuracy. Furthermore, a fixed number of samples can be used with smaller increments as is commonly used in the running average. Oversampling will result in azimuthal increments of data that are smaller than the width of the resolution volume, although the details provided by the raw data are still limited by the beamwidth.

Various researches have been conducted with the goal of improving the resolution of radar observations. Yu et al. (2006) developed a method for enhancing the range resolution using range-oversampled data, which involves the reprocessing of level-I data. Brown et al. (2002) and Brown et al. (2005) examined the impact of WSR-88D level-II data with "enhanced resolution" on the detection of tornado Doppler velocity signatures. Brown et al. (2002) have shown that the effective beamwidth can be reduced by a quarter by reducing the number of samples used in the estimation of spectral mo-

ments by half. Moreover, the azimuthal sampling interval is reduced by half given the same antenna rotation rate. As a result, stronger Doppler velocity signatures can be obtained at the expense of increasing the statistical variance of the moment estimates by a factor of 2.

In this paper, we propose an azimuthal oversampling technique, which, combined with a variational wind analysis, can provide flow structures that can be smaller in size than the radar beamwidth. Such additional details are particularly important to the detection of small-scale weather phenomena such as tornadoes. Note that in this work, the oversampled level-II data are obtained by processing the same number of samples as the one used in typical processing, but with smaller azimuthal increments. In other words, the data processing is similar to the procedure of running means. This approach will not degrade the statistical accuracy of moment estimates. The effective beamwidth is not reduced either as for the case of oversampling using a fewer number of samples (Brown et al. 2002). On the other hand, three-dimensional variational data assimilation (3DVAR) analysis will be exploited to retrieve subbeamwidth information, as will be described later. This method is tested and verified using a realistic model-simulated tornado vortex, and using reprocessed WSR-88D data for a real tornado case.

For the analysis of vector wind fields using radial velocity data, the availability of dual-Doppler radars is assumed. For such analyses, the variational technique is very effective, because it can easily incorporate the forward observation operators that involve, in our case, the beam pattern for the analyzed data. The method can also be used to effectively analyze single-Doppler radial velocity data when dual-Doppler coverage is not available. In addition, in regions with no radar observations, background values can be naturally combined with the radar data. Both the relative weighting of the background and observations and the smoothness of the analysis can also be effectively controlled (Gao et al. 1999, 2004a; Liu et al. 2004, 2005). For these reasons, a two-dimensional variational data assimilation (2DVAR) analysis procedure is applied to the analysis of oversampled radial velocity data at low levels in this study.

The paper is organized as follows. In section 2, the oversampling technique and wind analysis/retrieval method are described. The technique is then tested in section 3 using simulated data sampled from an ultrahigh-resolution numerical simulation of a tornado. In section 4, we further investigate the effectiveness of the technique by performing dual-Doppler wind analyses for a real tornado case observed by two WSR-88D radars (KTLX in Oklahoma City and a research WSR-

88D radar, KOUN, in Norman, Oklahoma). For KOUN, level-I data are reprocessed to generate over-sampled data at different azimuthal increments. Summary and conclusions are presented in section 5.

2. Radial velocity sampling and variational wind analysis

As discussed earlier, azimuthal oversampling can be achieved when the azimuthal increment of observations is smaller than the beamwidth. In our case, instead of using a smaller number of averaging samples or a slower antenna rotation rate, the spectral moments were estimated from the same number of samples as used in non-oversampling case with an azimuthal increment that is smaller than the beamwidth. For example, when the time interval between averaging operations is halved, an oversampling rate of two is resulted. The average radial velocity data thus obtained are effectively running means of the samples, and the averaged data represent the winds in regions that partially overlap. Because the same number of samples is used, the statistical accuracy of the moment estimates remains the same as that of non-oversampled data.

a. Radar data sampling and observation operator

For the purpose of variational wind analysis as well as for producing simulated observations from model simulation data, we need a “radar emulator” that samples an atmosphere defined at discrete grid points. In data assimilation terms, the formula of this emulator is called the forward observation operator, which turns gridpoint space state variables into the observed quantity. In our case, the gridpoint values are the Cartesian velocity components, and the observed quantity is the mean Doppler velocity. For simplicity, either the problem is assumed to be two-dimensional, or there is no variation in the vertical direction and the radar beams are horizontal. The same assumptions are made in Wood and Brown (1997), although our method and results can be easily generalized to three dimensions.

Following Wood and Brown (1997), we write the mean radial velocity $\bar{v}_r(\theta_0, r_0)$ for an effective radar volume centered at range r_0 and azimuth angle θ_0 as

$$\bar{v}_r(\theta_0, r_0) = \frac{\sum_i^I \sum_j^J v_r(\theta_i, r_j) |W(r_j)|^2 f^4(\theta_i)}{\sum_i^I \sum_j^J |W(r_j)|^2 f^4(\theta_i)}, \quad (1)$$

where I and J are, respectively, an odd number of grid points in the azimuth and range directions, centering at

the center of and spanning over the effective sampling volume; $v_r(\theta_i, r_j)$ is the radial velocity at point (θ_i, r_j) ; $|W(r)|^2$ is the magnitude of the two-way range-weighting function with a 6-dB width r_6 ; and $f^4(\theta)$ is the two-way antenna pattern with an effective half-power beamwidth θ_e . They are given by

$$|W(r_j)|^2 = \left(1 - \left|\frac{r_j - r_0}{r_6}\right|\right)^2, \quad (2)$$

$$f^4(\theta_i) = \exp\left[-4 \ln 4 \left(\frac{\theta_i - \theta_0}{\theta_e}\right)^2\right]. \quad (3)$$

Note that we assume that Eq. (3) has already taken into account the beam-broadening effect resulting from antenna rotation. For the radial velocity emulation purpose, the mean radial velocity data can be obtained in two steps. The first is to obtain individual radial velocity measurements or samples on a pulse-by-pulse basis, which uses the antenna pattern-weighting function with the physical half-power beamwidth. The second step averages a number of samples to obtain the mean or first-moment values. Such a pulse-by-pulse approach is taken by May et al. (2006, manuscript submitted to *J. Atmos. Oceanic Technol.*) in their more sophisticated radar emulator. For the practical purpose of data analysis and relatively simple forms of radar emulation, a single combined step using the above equations, with an effective beamwidth, provides a good approximation of the two-step process. The emulator is illustrated by Fig. 1.

b. Variational wind analysis

As mentioned earlier, we use a variational method to analyze the wind field on a high-resolution 2D grid from radial velocity data taken by two Doppler radars. The analysis grid interval is generally smaller than the non-oversampled data in crossbeam direction, and the analysis counts on the oversampling to recover sub-beamwidth flow details. The variational analysis minimizes a cost function that measures the distance both between the analysis and the observations, and between the analysis and a background or prior guess. In our case, an equation constraint is also included.

The actual cost function J is defined as

$$J = J^b + J^o + J^c, \quad (4)$$

where J^b is the background term, J^o is the observation term, and J^c is a weak divergence constraint.

The specific form of J^o is given by

$$J^o = \frac{1}{2} (\mathbf{V}_r^a - \mathbf{V}_r^o)^T \mathbf{R}^{-1} (\mathbf{V}_r^a - \mathbf{V}_r^o), \quad (5)$$

where $\mathbf{V}_r^o = \{v_r^o(\theta_0^m, r_0^m) | m = 1, 2, \dots, M\}$ is the vector of observed radial velocity and $v_r^o(\theta_0^m, r_0^m)$ denotes the

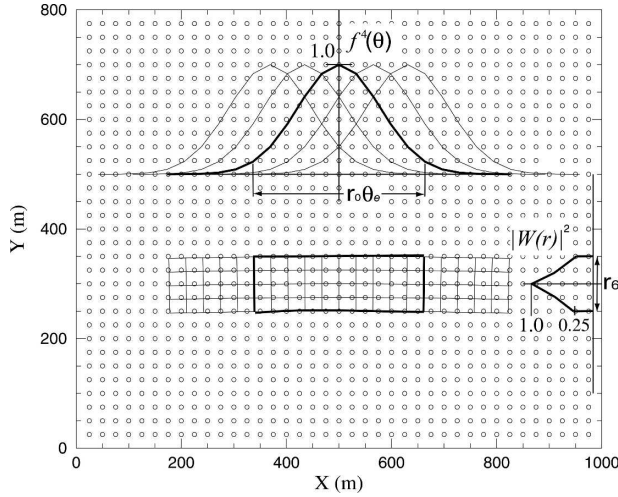


FIG. 1. Illustration of the simulation of radial velocity data from a gridded wind field, with azimuthal oversampling. The close circles in the figure represent the points of the analysis grid where velocity components u and v are defined. Radial velocity data are obtained by sampling this grid with a beam of a given effective beamwidth and range length, using Eq. (1). A number of overlapping sampling volumes are shown in the figure, at a sampling interval of 0.125° . The central sampling volume is highlighted in bold. The weighting functions in range (W^2) and in azimuth (f^4) are plotted to the right and above the example overlapping sampling volumes, respectively.

radial velocity observations from all radars, with superscript m denoting the m th radar measurement and M the total number of observations. Here $\mathbf{V}_r^a = \{v_r^a(\theta_0^m, r_0^m) | m = 1, 2, \dots, M\}$ is the radial velocity vector corresponding to the analyzed wind field, and its individual element $v_r^a(\theta_0^m, r_0^m)$ is linked by the same equation as given in (1) to $v_r^a(\theta_i^m, r_j^m)$, the radial velocity values at the grid points within the effective sampling volume in the radar polar coordinates. The $v_r^a(\theta_i^m, r_j^m)$ is in turn related to the x and y wind components $u^a(\theta_i^m, r_j^m)$ and $v^a(\theta_i^m, r_j^m)$ at the same points by

$$v_r^a(\theta_i^m, r_j^m) = \cos(\theta_i^m)u^a(\theta_i^m, r_j^m) + \sin(\theta_i^m)v^a(\theta_i^m, r_j^m), \quad (6)$$

where $u^a(\theta_i^m, r_j^m)$ and $v^a(\theta_i^m, r_j^m)$ are bilinearly interpolated from the analyzed wind components on the Cartesian analysis grid. In Eq. (5), \mathbf{R} is the observation error covariance matrix and is assumed, as is commonly done, to be diagonal in this paper, that is, the observation errors are assumed to be uncorrelated.

The background term in (4) is given by

$$J^b = \frac{1}{2}(\mathbf{u}^a - \mathbf{u}^b)^T \mathbf{B}_u^{-1}(\mathbf{u}^a - \mathbf{u}^b) + \frac{1}{2}(\mathbf{v}^a - \mathbf{v}^b)^T \mathbf{B}_v^{-1}(\mathbf{v}^a - \mathbf{v}^b), \quad (7)$$

where \mathbf{u}^a and \mathbf{v}^a are the analyzed wind component vectors on the Cartesian analysis grid, \mathbf{u}^b and \mathbf{v}^b are the corresponding background vectors or prior estimates, and \mathbf{B}_u and \mathbf{B}_v are the background error covariance matrices for \mathbf{u} and \mathbf{v} , respectively. Here we assume that the background errors in \mathbf{u} and \mathbf{v} are uncorrelated, and the spatial error covariances are assumed Gaussian and modeled using a recursive spatial filter (Hayden and Purser 1995; Purser et al. 2003; Gao et al. 2004b; Liu and Xue 2006). The diagonal elements of \mathbf{B} are the error variances of the background field.

The divergence equation constraint is given by

$$J^c = \frac{1}{2} \left(\frac{\partial \mathbf{u}}{\partial x} + \frac{\partial \mathbf{v}}{\partial y} \right)^T \mathbf{Q}^{-1} \left(\frac{\partial \mathbf{u}}{\partial x} + \frac{\partial \mathbf{v}}{\partial y} \right), \quad (8)$$

where \mathbf{Q} is the equation error covariance matrix, which is also assumed diagonal in this paper.

The key difference of our variational analysis procedure from earlier work (e.g., Gao et al. 1999; Liu et al. 2004) lies with the use of a sophisticated forward observation operator that closely simulates the way in which a scanning Doppler radar samples the atmosphere. Further, the use of an analysis grid resolution that is comparable to the intervals of oversampled velocity measurements potentially allows for the recovery of flow structures that are smaller than the beamwidth.

3. Tests with simulated radar data

In this section, we test the ability of our variational analysis procedure in producing detailed flow analysis from simulated radar observations with and without azimuthal oversampling.

a. The simulation of radial velocity data

A high-resolution simulation of a supercell storm with an embedded F4–F5 intensity tornado is used as the “true” atmosphere on which simulated radar data are collected. This simulation was performed using the Advanced Regional Prediction System (ARPS; Xue et al. 2000, 2001), which is a fully compressible and non-hydrostatic prediction model that predicts wind components u , v , w , potential temperature θ , pressure p , the mixing ratios for water vapor, and microphysical species. The current simulation used the Kessler-type warm-rain microphysics. The model thunderstorm was initiated by an artificial thermal bubble in an initially horizontally homogeneous environment defined by a sounding for the 20 May 1977 Del City, Oklahoma, supercell storm case (Ray et al. 1981).

A uniform horizontal resolution of 50 m was used over a $48 \text{ km} \times 48 \text{ km}$ domain, together with a vertical

stretched grid with a near-surface vertical resolution of 20 m. The simulation time was over 4 h. Over a half-hour period centering on the time of the most intense tornado obtained on the 50-m grid, a simulation using a 25-m resolution is performed, starting from an initial condition interpolated from the 50-m grid. On this grid, a maximum ground-relative wind speed of over 120 m s^{-1} was obtained, with a pressure drop of over 80 hPa at the center of the tornado vortex. Detailed description and analyses of the simulations will be reported elsewhere. In this paper, we will use a single time level output from this 25-m simulation as input to our radar emulator to create simulated observations. From these observations, variational wind analyses are performed and compared with the truth. In particular, Eq. (1) is used to collect simulated data with and without oversampling.

The two radars are located due west and south of the analysis grid, and their distances from the domain center depend on experiment. As mentioned earlier, we evaluate our oversampling strategy in two dimensions only, and assume that radar beam elevation is 0° and ground clutters are not considered. The analysis grid therefore corresponds to the surface level of the simulation grid. The impacts of the azimuthal increments of oversampling, the distance of the radars from the tornado, and the effective beamwidth on the wind analysis are examined.

b. Wind analyses with different azimuthal oversampling

In the first set of experiments, the distance from the center of analysis domain is 15 km for both radars, the range resolution [r_6 is Eq. (2)] is 100 m, and the effective beamwidth is assumed to be 2° . The azimuthal increment is set to different values ranging from 0.125° to 2° . The 2° effective beamwidth is roughly that of the CASA Oklahoma test bed radars, and the 0.125° increment represents a factor-of-16 oversampling. As with all experiments, the analysis domain is $9 \text{ km} \times 9 \text{ km}$, the analysis variables are the u and v components, and the grid resolution is 25 m; the grid therefore has 361×361 points. The recursive filter scale, or the spatial decorrelation length of the background error, is set to five grid intervals, which gives a decorrelation radius of 125 m and is somewhat larger than the gate spacing of 100 m. This ensures a smooth analysis between gates, although the averaging in the emulator resulting from the radial beam pattern also acts to fill the gaps between data in the radial direction. A zero velocity value is assumed for the analysis background; therefore a rather large value of background error variance of $400 \text{ m}^2 \text{ s}^{-2}$ is used based on the assumption that the average wind speed is about 20 m s^{-1} . The error variance for

the divergence constraint term is set to 0.2 s^{-2} , which is chosen based on numerical experimentations. This effectively nondivergent constraint is most important where there is only single-Doppler velocity coverage; it acts to provide crossbeam information from the radial wind measurements.

The simulated low-level radial velocity fields by the radar located 15 km from the center of analysis domain on the south side are shown Fig. 2 for azimuthal increments of 0.125° , 1° and 2° , respectively. As can be seen, the resolution of the radial velocity field is rather poor when the azimuthal increment is 2° , which represents the non-oversampling case, and the maximum gate-to-gate velocity difference (Mitchell et al. 1998) of the radial velocity couplet associated with the tornado (located approximately at $x = -0.3$, $y = 16 \text{ km}$), is only 12 m s^{-1} (Fig. 2c). With a 0.125° increment, the maximum gate-to-gate velocity difference at the tornado location decreases to about 8 m s^{-1} , but the maximum radial velocity difference across the tornado vortex is larger ($\sim 20 \text{ m s}^{-1}$) because in this case the maximum difference now occurs across several gates in azimuth. The averaging resulting from the broad effective beam is the main reason for the rather weak observed shear in both cases. Apparently, decreasing the azimuthal increment without decreasing the beamwidth can actually lead to smaller gate-to-gate shear magnitude.

The adjacent or gate-to-gate velocity difference is a key criterion for identifying tornado from radar data (Mitchell et al. 1998; Liu et al. 2007). Too small an adjacent velocity difference will result in a failure in tornado detection. When the azimuthal increment is decreased to 0.125° , the radial velocity field contains much more details (Fig. 2a), although the gate-to-gate velocity difference remains low. The characteristics of the radial velocity fields with different azimuthal increments from the radar on the west side (not shown) are similar to those shown in Fig. 2. It is clear that azimuthal oversampling is helpful, but as will be shown that it takes a "deconvolution" process involved in the variational analysis to uncover the subbeam flow structures.

Figure 3 shows, together with the true wind fields, the wind vector, u , and v fields analyzed from the data of the two radars, sampled at 0.125° and 2° azimuthal increments. The results show that the major features of the tornado vortex are well captured by the analysis using data oversampled at 0.125° increments. In particular, the tornado circulation analyzed from the oversampled data (Fig. 3f) is much tighter; it has a radius of about 250 m, which is very similar to the true field. The vortex analyzed from non-oversampled data is much

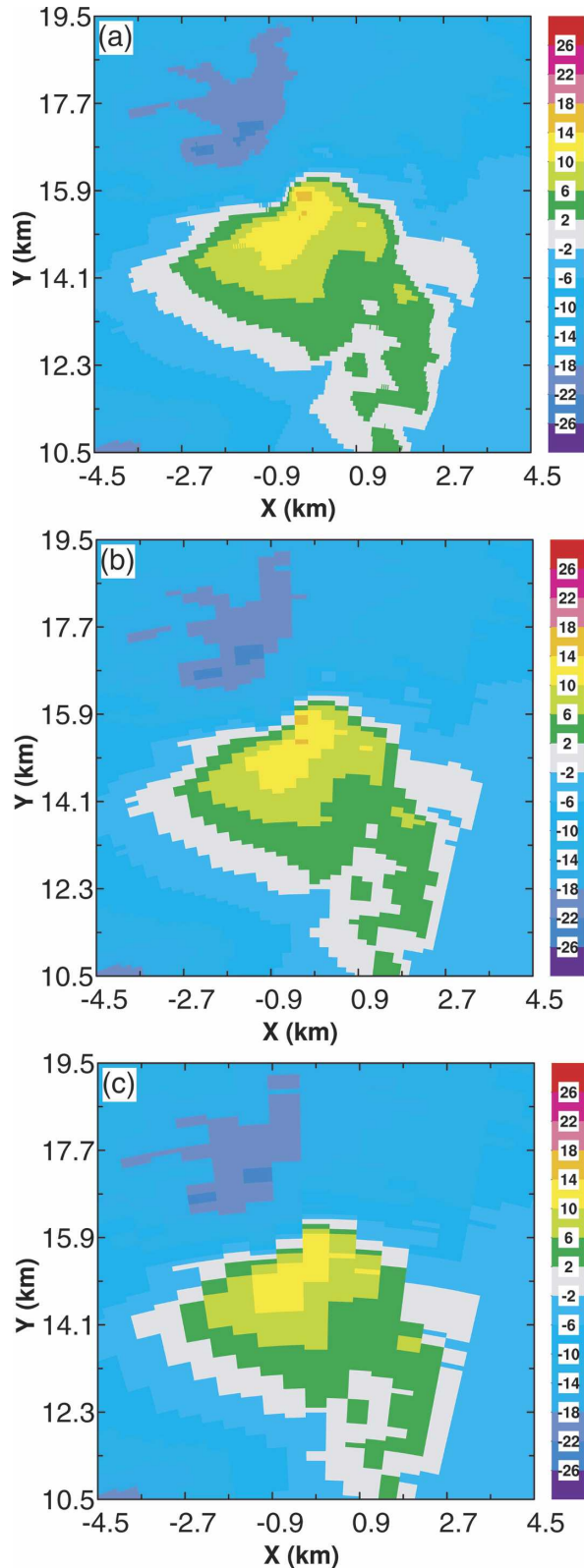


FIG. 2. Simulated radial velocity fields from the radar located at (0, 0) km, or 15 km south of the 9 km \times 9 km analysis domain center with azimuthal increments of (a) 0.125°, (b) 1°, and (c) 2°.

weaker and broader, and the vortex circulation is somewhat discontinuous along its circle. The shears in terms of both u and v components are much stronger for the oversampled case (Figs. 3d,f) than the non-oversampled case (Figs. 3g,h). The velocity couplet in u has a maximum shear of over 40 m s⁻¹ in the former case, while in the latter this is about 35 m s⁻¹ and the distance between the couplet centers is about 500 m instead of about 700 m of the oversampled case. The maximum shear in the true field (Fig. 3a) is more than 55 m s⁻¹, and the distance between the couplet centers is less than 300 m. The differences between the analyzed v fields are even larger (Figs. 3e,h), with that from oversampled data being much closer to the truth (Fig. 3b). We note that in this case, the azimuthal width of the radar beam at the location of tornado is about 500 m, which is wider than the 300-m core radius of the tornado vortex.

To quantitatively evaluate the accuracy of the analysis fields, especially in terms of the spatial structure of the flow, the correlation coefficients (CCs) between the true and the analyzed vector wind fields are calculated for each experiment according to

$$CC = \frac{\Sigma(\mathbf{V}^a - \bar{\mathbf{V}}^a)(\mathbf{V}^t - \bar{\mathbf{V}}^t)}{\sqrt{\Sigma(\mathbf{V}^a - \bar{\mathbf{V}}^a)^2 \Sigma(\mathbf{V}^t - \bar{\mathbf{V}}^t)^2}}, \quad (9)$$

where \mathbf{V}^a and \mathbf{V}^t are the analyzed and true vector winds, respectively, and the overbar denotes domain average. The summation is over all the grid points in the analysis domain. The correlation coefficients for the above two experiments as well as three other experiments with intermediate values of azimuthal increments are given in Table 1. As can be seen, the CC steadily increases from the 0.68 for the non-oversampled case (2° increment) to the 0.91 in the case of 0.125° increment, a certainly significant improvement. These results clearly demonstrate that the variational analysis procedure is able to recover detailed information of the flow structures contained in the oversampled radial velocity data, when two radars sample the tornado circulation at a distance of about 15 km and at a right angle to each other. Quality analysis of the tornado vortex is obtained, with a correlation coefficient reaching 0.91 with a 16 times oversampling.

c. Impact of radar range on wind analysis

Because the effective sampling volume of radar data increases with the distance from the radar, the azimuthal data resolution decreases as a result. The effects of the distance of the tornado from the radars on the wind analyses are assessed by a set of experiments in which the tornado is located 12, 15, 18, 21, and 24 km

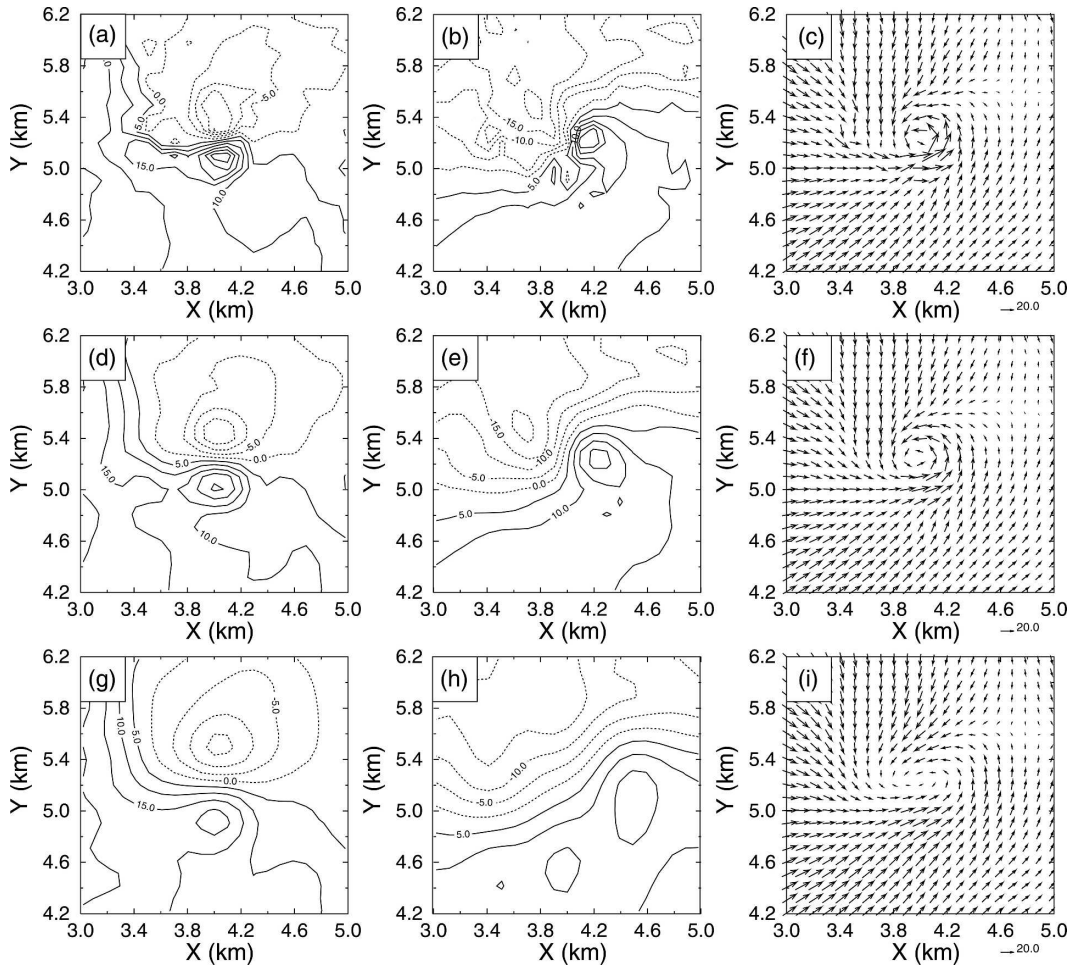


FIG. 3. The u and v contours and vectors of (a)–(c) “true,” and analyzed winds from oversampled radial velocity data with azimuthal increments of (d)–(f) 0.125° and (g)–(i) 2° . The effective beamwidth is 2° and the radars are about 15 km from the center of analysis domain on the west and south side. Only a portion of the $9 \text{ km} \times 9 \text{ km}$ analysis domain is shown and the coordinate origin is at the southwest corner of the analysis domain.

from both radars. These experiments are performed for both azimuthal increments of 0.125° and 2° with an effective beamwidth of 2° . The 15-km distance experiments are the same as those shown earlier. The CCs of the analyzed vector wind fields are given in Table 2. As expected, the farther the radars are from the tornado, the poorer is the analysis of tornado circulation. It is interesting that at a distance of 24 km, 4/5 of the maximum designed range of the CASA radars (of 30 km), the oversampled analysis is still significantly better (CC = 0.76) than that obtained from non-oversampled

data taken at half of the range (12 km). The wind fields analyzed from data with 0.125° and 2° azimuthal increments, when both radars are about 24 km from the tornado, are plotted in Fig. 4. As can be seen from Figs. 4a–c, a strong closed tornado vortex is obtained in the analysis with oversampled data while a closed circulation is absent in the analysis with non-oversampled data (Fig. 4f). Clearly, oversampling is able to mitigate quite effectively the resolution degradation with range, and

TABLE 1. CCs for different azimuthal increments when the radars are located 15 km from the center of the analysis domain.

Azimuthal increment	0.125	0.5	1.0	1.5	2.0
CC	0.90	0.82	0.78	0.72	0.68

TABLE 2. Correlation coefficients of the analyses when the radars are located at different distances from the center of analysis domain, for azimuthal increments of 0.125° and 2° .

Distance	12.0	15.0	18.0	21.0	24.0
Azimuthal increment 0.125°	0.92	0.90	0.83	0.82	0.76
Azimuthal increment 2°	0.71	0.69	0.66	0.65	0.56

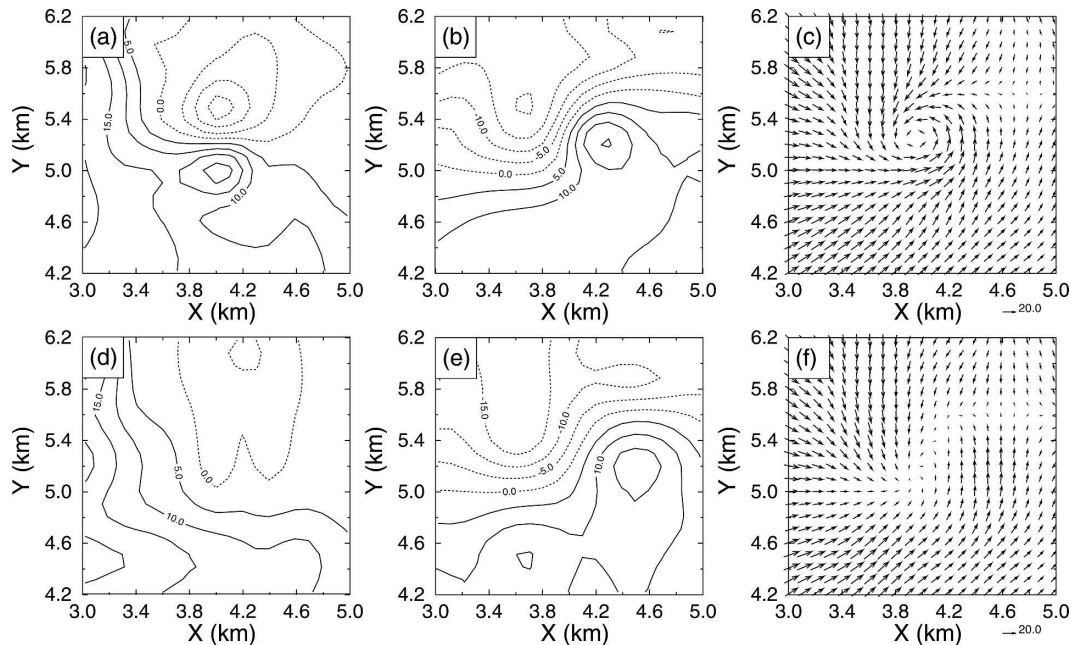


FIG. 4. The analyzed winds from radial velocity data sampled at (a)–(c) 0.125° and (d)–(f) 2.0° azimuthal increments. The effective beamwidth is 1° . Both radars are about 24 km from the center of analysis domain, on the west and south side.

alleviate the effect of relatively wide beams. The root-mean-square errors of the analyses were also calculated and are consistent with those from the correlation coefficients.

d. Impacts of effective beamwidth

In all earlier experiments, we assumed an effective beamwidth of 2° , roughly corresponding to that of the CASA Oklahoma test bed radars. For the WSR-88D radars, the physical beamwidth is roughly 1° . It is of interest to investigate how much the analysis is improved with a narrower beam. In general, the smaller the effective beamwidth, the more detailed flow structure the data can capture.

Results from two experiments with data sampled at a 1° effective beamwidth for both radars are presented with an azimuthal increment of 0.125° , or a factor-of-8 oversampling. Other settings of the experiments are the same as those experiments in section 3b.

The analyzed fields are shown in Fig. 5. As shown, with a narrower beamwidth, even more detailed wind structure is captured. In Fig. 5b, the maximum shear in terms of the v component is noticeably stronger ($\sim 45 \text{ m s}^{-1}$) than the corresponding one in the 2° beamwidth case ($\sim 40 \text{ m s}^{-1}$; cf. Fig. 3e), while that in terms of u exceeds 55 m s^{-1} (Fig. 5a). The analyzed wind vector field (Fig. 5c) looks remarkably similar to the truth (Fig. 3c), including small-scale details. The CC between

the analysis and truth is a remarkable 0.95 and is 5% higher than the 0.90 of the corresponding 2° beamwidth case (Table 1). These results indicate that, with a 1° beamwidth, a 15-km observing distance, and a factor-of-8 oversampling, the analysis of a tornado on a 25-m resolution grid is able to essentially fully recover the flow details associated with the tornado simulated at the same resolution, even though near the tornado the width of the beam is about 250 m and the range resolution is 100 m. The azimuth oversampling obviously plays an important role here.

4. Tests with real radar data

The simulated data used in the previous tests contained no explicitly added error. As discussed in section 2, because the same number of samples as that of the conventional scheme was used, the statistical errors of these data should be the same as that of non-oversampled data. For the simulated data, the pulse averaging was not explicitly performed. In this section, we test the effectiveness of the oversampling and analysis procedure by using oversampled data processed from level-I data from one of two WSR-88D radars observing a real tornadic thunderstorm.

a. Case description and radar data processing

Radar data collected by the Oklahoma City WSR-88D radar (KTLX) and the National Severe Storms

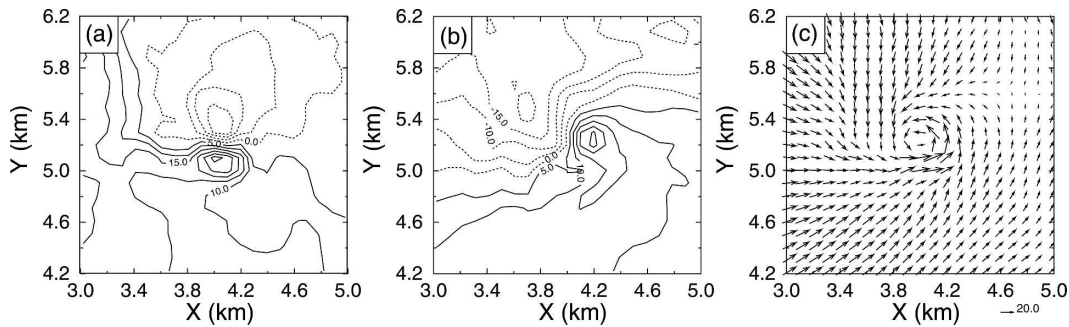


FIG. 5. The (a) u and (b) v contours and (c) vectors of the analyzed winds from oversampled radial velocity data with an azimuthal increment of 0.125° and an effective beamwidth of 1° .

Laboratory (NSSL) research dual-polarization WSR-88D radar in Norman, Oklahoma (KOUN) on 10 May 2003 are used. On that day, nine tornadoes were produced from 0150 to 0425 UTC by a supercell that was initiated along a dryline. The tornado presented in this work formed at 0310 UTC about 28 km north of the KOUN radar and 38 km south-southwest of KTLX radar. The tornado reached an F1 intensity by 0310 UTC, but dissipated by 0314 UTC. The tornado traveled for about 3.8 km on the ground. This tornado was observed by both KOUN and KTLX radars in the lowest elevation.

The level-I data from KOUN radar were reprocessed to produce oversampled radial velocity data at up to a 0.125° azimuthal increments using the method described in section 2. The radial velocity data from both radars passed through radar data quality control (Liu et al. 2003). The radial velocity fields from KOUN with and without oversampling, and that from KTLX radar, are shown in Fig. 6 for the lowest elevation. The oversampled radial velocity field of KOUN (Fig. 6b) shows more velocity structures and stronger wind shears near the tornado than in the non-oversampled case (Fig. 6c). In Figs. 6b,c the tornado centers revealed by the data are not exactly at the same location, because of the difference in azimuthal resolutions.

b. Results of analysis

The variational analysis algorithm is applied to the real case. The analysis domain is $10 \text{ km} \times 10 \text{ km}$ in size and has 401×401 grid points at a 25-m resolution. The analysis variables are u and v wind components. The coordinate origin is set at the lower left or southwest corner of the analysis domain, so that KOUN is located at $(2.7, -32.70)$ km and KTLX at $(17.55, -23.05)$ km. Because the gate interval for both KTLX and KOUN is 250 m, the filter scale is chosen to be 10 grid intervals so

that the gaps between observations can be covered. Within the analysis domain, there are few observation regions where the angle between two radar beams is larger than 30° . This is a less-than-ideal situation, and the small angles between dual-Doppler velocity data can potentially lead to large analysis errors. In addition, we assumed that all data from the two radars lie within the same 2D analysis plane, an approximation that can also lead to analysis errors.

Because the scan times of two radars are not exactly the same and the tornado propagated quickly, time correction to the radar observations is necessary. An advection correction technique (Gal-Chen 1982; Liu et al. 2004) is used in this paper. The advection speed is estimated based on the tornado center locations identified from the oversampled KOUN and the KTLX data. The tornado center locations identified from KTLX is shifted to the center identified from oversampled KOUN data. Using the shift distance and time difference between the two scans, the moving-frame velocity components are estimated as 13.3 and 6.6 m s^{-1} in the x and y directions, respectively. This speed is used in the advection correction.

In the first experiment, oversampled radial velocity from KOUN together with regular KTLX data are used, while in the second experiment regular KOUN data are used. The results are shown in Fig. 7. The upper panel shows the u and v contours and wind vector field of the analyzed winds from the first experiment, while those from the second experiment are shown in the lower panel. As shown, a tornado cyclone is revealed by both analyses. There are strong wind shears near the tornado center in both u and v components, and a vortex circulation can be clearly identified from the vector wind fields (Figs. 7c and 7f) also.

However, the tornado circulation in the analysis with oversampled data is much stronger. The u and v fields show much stronger shear in the oversampling case

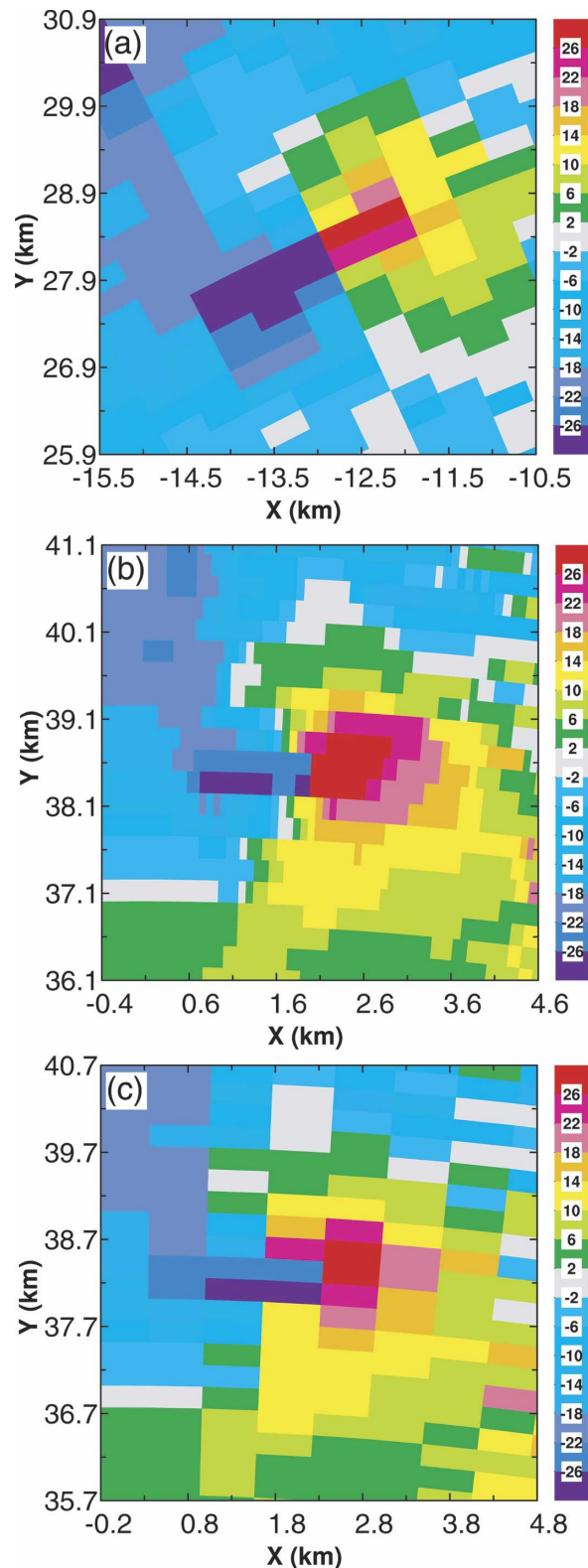


FIG. 6. The radial velocity fields (a) from the KTLX radar and from KOUN radar with azimuthal increments of (b) 0.125° and (c) 1° for the lowest elevation. The origin of the coordinate is set to location of radar for both cases.

(Figs. 7a and 7b). The minimum u is less than -40 m s^{-1} and the maximum is greater than 60 m s^{-1} in Fig. 7a, while the corresponding numbers of the non-oversampling case are -15 and 25 m s^{-1} , respectively (Fig. 7d). The magnitudes of the minimum and maximum v are also larger in the oversampling case (cf. Figs. 7b and 7e). The tornado circulation in the oversampling case is also clearly tighter (Fig. 7c). While the truth of the real tornado circulation is unknown, the general circulation features of the analyzed tornado in the oversampling case are closer to those of numerically simulated tornado shown earlier.

The vector wind field in Fig. 7c contains more detailed flow structures than in Fig. 7f. North of the tornado center, there is a region of strong divergent flow, while on the northwest side of the tornado, there is a region of strong convergent inflow. The existence of convergence inflow to the northwest side that feeds into the tornado suggests the importance of downdraft in tornadogenesis (Davies-Jones et al. 2001) and is consistent with the findings from recent high-resolution numerical simulations performed by the first author.

Note that the convergence shown in Fig. 7c may be too strong because of the large analyzed u in that region. This large u may not be completely realistic because the projection of the observed radial winds from both radars is small in this direction.

5. Summary and conclusions

In this paper, an azimuthal oversampling technique and a variational analysis scheme are developed for retrieving finescale flow structures that can be smaller than the radar beamwidth. The oversampled data are obtained by performing a running mean of consecutive pulse samples collected by a rotating antenna. To retain a sufficient level of data accuracy, the same number of samples is used in the moment processing as is typically used to obtain the non-oversampled data. In the variational analysis, a forward observation operator that simulates how the real data are obtained is used, which enables the analysis system to “recover” subbeam-scale structures contained within the data at subbeamwidth intervals.

The effectiveness of our proposed data processing and analysis procedure is first tested using simulated data for a case of model-simulated tornado, then using reprocessed data for a real observed tornado, for which dual-Doppler data are available.

In the simulated data tests, radial velocity data are sampled from a 25-m resolution simulation of an intense tornado embedded within a supercell, using a re-

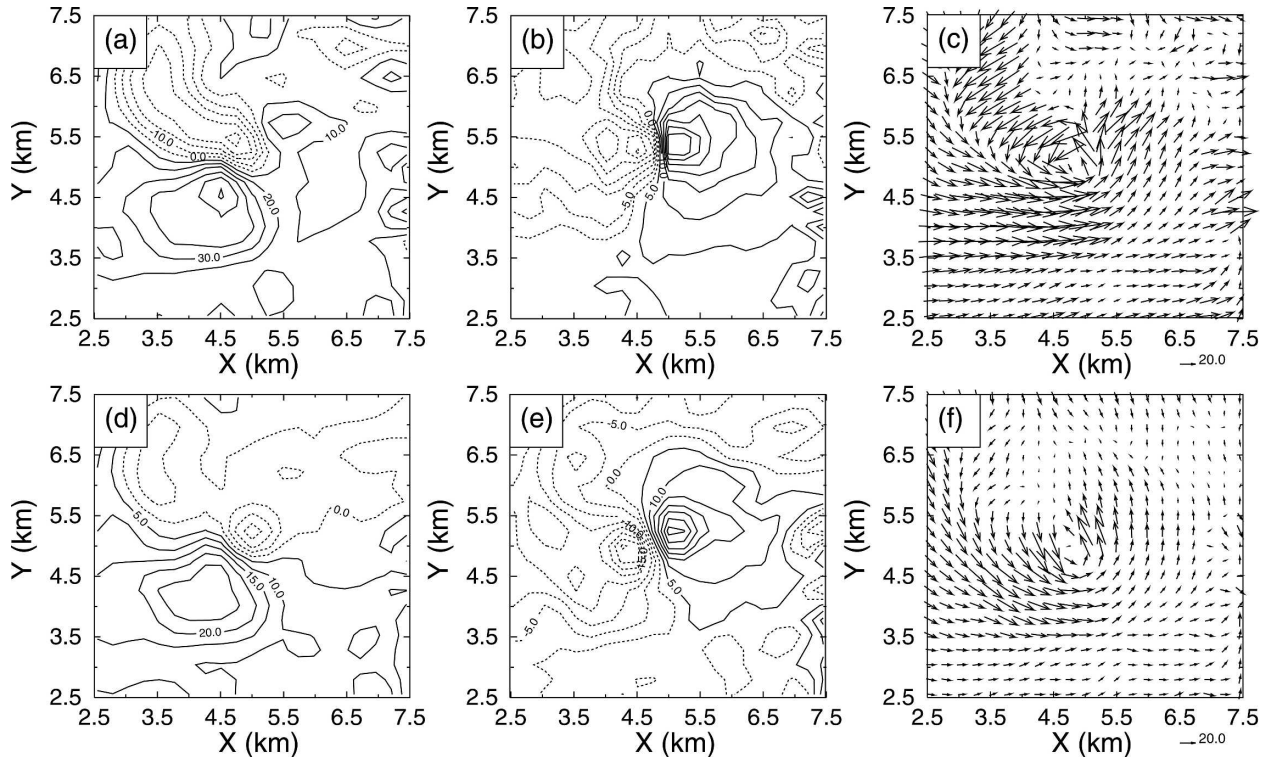


FIG. 7. The u (a), (d) and v (b), (e) contours and vectors of analyzed winds (c), (f) from the regular KTLX data, and the KOUN data (a)–(c) with and (d)–(f) without oversampling. An azimuth increment of 0.125° is used in the oversampled case.

alistic radial velocity emulator. The impacts of the azimuthal oversampling increment and of the distance of the tornado from the radars are examined. When the azimuthal oversampling increment decreases the wind retrieval is improved. When the distance between the tornado and the radars is larger, the retrieval results become worse; however, it is shown that using azimuthal oversampling and the variational analysis algorithm together can help overcome the negative impact of the increasing width of radar beams when the radars are located further away from the tornado. With the simulated data, the effects of effective beamwidth in the variational analysis are also tested.

For the real data tests, we reprocessed the level-I data from the KOUN radar for the 10 May 2003 central Oklahoma tornadic thunderstorm case. The oversampled data are analyzed together with regular radial velocity data from the Oklahoma City WSR-88D radar (KTLX). The intensity of the retrieved tornado vortex using oversampled data is significantly higher than that obtained without oversampling. Low-level flow structures that are consistent with recent high-resolution simulations of supercell tornadoes are obtained, suggesting the potential of our technique in diagnostic studies of real tornadoes.

In practice, the data processing associated with data oversampling can be performed at the radar site, requiring some increase in the computer processing power but no modifications to the radar hardware. If our main interests are in the detection of low-level features, such as tornadoes and downbursts, this oversampling data processing can be performed for the lower elevations only. While the proposed oversampling strategy may not be completely new, it is the proposed variational analysis procedure that allows for the recovery of subbeamwidth structures. Through the variational analysis, much greater benefits can be realized with oversampling. Finally, we realize that the amount of testing with real data is still rather limited; future collection of oversampled dual-Doppler data using, for example, the CASA radars, is planned to further evaluate our method.

Finally, we point out that our analysis system can be extended to three dimensions with relative ease, and by including a 3D mass continuity equation as a weak constraint, as is done in Gao et al. (1999), the analysis of all three wind components can be obtained. Such analyses will be valuable for many purposes, including understanding tornado dynamics.

Acknowledgments. This work was primarily supported by NSF Grant EEC-0313747 of the Engineering Research Center (ERC) Program to the Center for Collaborative Adaptive Sensing of Atmosphere (CASA). S. Liu and M. Xue were also supported by an FAA Grant via DOC-NOAA NA17RJ1227, and M. Xue further by NSF Grants NSF ATM-0530814, ATM-0331594, and ATM-0331756. T. Y. Yu was supported by NOAA CSTAR Grant NJ17RJ1227. The authors would also like to acknowledge the technical support from NSSL for collecting the level-I time series data.

REFERENCES

- Brotzge, J. A., K. Brewster, B. Johnson, B. Philips, M. Preston, D. Westbrook, and M. Zink, 2005: CASA's first testbed: Integrated project #1 (IP1). Preprints, *32d Conf. on Radar Meteorology*, Albuquerque, NM, Amer. Meteor. Soc., CD-ROM 14R.2.
- Brown, R. A., V. T. Wood, and D. Sirmans, 2002: Improved tornado detection using simulated and actual WSR-88D data with enhanced resolution. *J. Atmos. Oceanic Technol.*, **19**, 1759–1771.
- , B. A. Flickinger, E. Forren, D. M. Schultz, D. Sirmans, P. L. Spencer, V. T. Wood, and C. L. Ziegler, 2005: Improved detection of severe storms using experimental fine-resolution WSR-88D measurements. *Wea. Forecasting*, **20**, 3–14.
- Crum, T. D., R. L. Alberty, and D. W. Burgess, 1993: Recording, archiving, and using WSR-88D data. *Bull. Amer. Meteor. Soc.*, **74**, 645–653.
- Davies-Jones, R., R. J. Trapp, and H. B. Bluestein, 2001: Tornadoes and tornadic storms. *Severe Convective Storms*, C. A. Dowswell III, Ed., Amer. Meteor. Soc., 167–222.
- Doviak, R., and D. Zrnica, 1993: *Doppler Radar and Weather Observations*. 2d ed. Academic Press, 562 pp.
- Gal-Chen, T., 1982: Errors in fixed and moving frame of references: Applications for convective and Doppler radar analysis. *J. Atmos. Sci.*, **39**, 2279–2300.
- Gao, J.-D., M. Xue, A. Shapiro, and K. K. Droegemeier, 1999: A variational method for the analysis of three-dimensional wind fields from two Doppler radars. *Mon. Wea. Rev.*, **127**, 2128–2142.
- , —, K. Brewster, and K. K. Droegemeier, 2004a: A three-dimensional variational data analysis method with recursive filter for Doppler radars. *J. Atmos. Oceanic Technol.*, **21**, 457–469.
- , M. Xue, K. Brewster, and K. K. Droegemeier, 2004b: A three-dimensional variational data analysis method with recursive filter for Doppler radars. *J. Atmos. Oceanic Technol.*, **21**, 457–469.
- Hayden, C. M., and J. Purser, 1995: Recursive filter objective analysis of meteorological fields: Applications to NESDIS operational processing. *J. Appl. Meteor.*, **34**, 3–15.
- Liu, H., and M. Xue, 2006: Retrieval of moisture from slant-path water vapor observations of a hypothetical GPS network using a three-dimensional variational scheme with anisotropic background error. *Mon. Wea. Rev.*, **134**, 933–949.
- Liu, S., P. Zhang, L. Wang, J. Gong, and Q. Xu, 2003: Problems and solutions in real-time Doppler wind retrievals. Preprints, *31st Conf. on Radar Meteorology*, Seattle, WA, Amer. Meteor. Soc., 308–309.
- , C. Qiu, Q. Xu, and P. Zhang, 2004: An improved time interpolation for three-dimensional Doppler radar wind analysis. *J. Appl. Meteor.*, **43**, 1379–1391.
- , —, —, —, J. Gao, and A. Shao, 2005: An improved method for Doppler wind and thermodynamic retrievals. *Adv. Atmos. Sci.*, **21**, 90–102.
- , M. Xue, and Q. Xu, 2007: Using wavelet analysis to detect tornadoes from Doppler radar radial-velocity observations. *J. Atmos. Oceanic Technol.*, **24**, 344–359.
- Mitchell, E. D., S. V. Vasiloff, G. J. Stumpf, A. Witt, M. D. Eilts, J. T. Johnson, and K. W. Thomas, 1998: The national severe storms laboratory tornado detection algorithm. *Wea. Forecasting*, **13**, 352–360.
- Purser, R. J., W.-S. Wu, D. F. Parrish, and N. M. Roberts, 2003: Numerical aspects of the application of recursive filters to variational statistical analysis. Part I: Spatially homogeneous and isotropic Gaussian covariances. *Mon. Wea. Rev.*, **131**, 1524–1535.
- Ray, P. S., B. Johnson, K. W. Johnson, J. S. Bradberry, J. J. Stephens, K. K. Wagner, R. B. Wilhelmson, and J. B. Klemp, 1981: The morphology of severe tornadic storms on 20 May 1977. *J. Atmos. Sci.*, **38**, 1643–1663.
- Wood, V. T., and R. A. Brown, 1997: Effects of radar sampling on single-Doppler velocity signatures of mesocyclones and tornadoes. *Wea. Forecasting*, **12**, 928–938.
- Xue, M., K. K. Droegemeier, and V. Wong, 2000: The Advanced Regional Prediction System (ARPS)—A multiscale nonhydrostatic atmospheric simulation and prediction tool. Part I: Model dynamics and verification. *Meteor. Atmos. Phys.*, **75**, 161–193.
- , and Coauthors, 2001: The Advanced Regional Prediction System (ARPS)—A multiscale nonhydrostatic atmospheric simulation and prediction tool. Part II: Model physics and applications. *Meteor. Atmos. Phys.*, **76**, 143–165.
- , M. Tong, and K. K. Droegemeier, 2006: An OSSE framework based on the ensemble square-root Kalman filter for evaluating impact of data from radar networks on thunderstorm analysis and forecast. *J. Atmos. Oceanic Technol.*, **23**, 46–66.
- Yu, T., G. Zhang, A. B. Chalamalasetti, R. J. Doviak, and D. Zrnica, 2006: Resolution enhancement technique using range oversampling. *J. Atmos. Oceanic Technol.*, **23**, 228–240.